

# Protonation of Chlorine Nitrate and Nitric Acid: Identification of Isomers by Vibrational Spectroscopy

Jong-Ho Choi,<sup>†</sup> Keith T. Kuwata, Yi-Bin Cao, Bernd-Michael Haas,<sup>‡</sup> and Mitchio Okumura\*

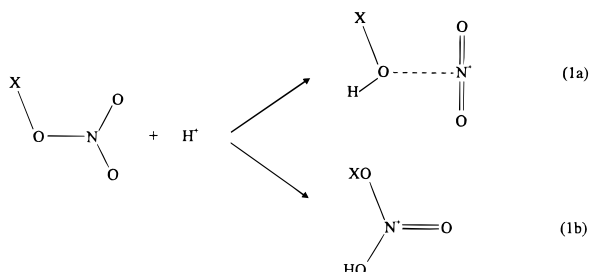
Arthur Amos Noyes Laboratory of Chemical Physics, California Institute of Technology, Pasadena, California 91125

Received: February 28, 1997; In Final Form: May 14, 1997<sup>⊗</sup>

Predissociation spectra in the 2.6–3.3  $\mu\text{m}$  region were observed for protonated chlorine nitrate and protonated nitric acid as well as some of their isotopomers ( $\text{HXNO}_3^+$ ,  $\text{X} = \text{H}, \text{D}, {}^{35}\text{Cl}, {}^{37}\text{Cl}$ ). Two protonated isomers of both  $\text{ClONO}_2$  and  $\text{HNO}_3$  were identified from the vibrational spectra. The lowest energy isomer was the ion–molecule complex  $\text{NO}_2^+(\text{HOX})$  formed by protonation of the XO group. The second isomer was the metastable species  $(\text{HO})(\text{XO})\text{NO}^+$  formed by protonation of a terminal oxygen; this isomer was generated only under hotter ionizing conditions. The vibrational band centers of these isomers agreed well with *ab initio* predictions. Vibrational excitation of the  $\text{HXNO}_3^+$  species studied here led solely to  $\text{NO}_2^+ + \text{HOX}$  products. Predissociation of the covalently bound metastable isomers  $(\text{HO})(\text{XO})\text{NO}^+$  to these products required an IR-induced rearrangement involving simultaneous 1,3 hydrogen shift and charge transfer. The results presented here were consistent with predictions of *ab initio* calculations and previous mass spectrometric and kinetic studies.

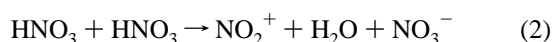
## 1. Introduction

The protonation of nitrate-containing molecules  $\text{XONO}_2$  can proceed by attack of either the XO group or one of the terminal O atoms:



Protonation of the XO site to form the ion–molecule adduct  $\text{NO}_2^+(\text{XOH})$  is generally the most exothermic channel because the nitronium ion, which is isoelectronic with  $\text{CO}_2$ , is very stable. The covalently bound isomers produced by protonation of a terminal oxygen atom are also expected to be bound though possibly metastable. In this paper, we present spectroscopic evidence for isomers of two protonated nitrates, protonated nitric acid,  $\text{H}_2\text{NO}_3^+$ , and protonated chlorine nitrate,  $\text{HClONO}_2^+$ .

Nitrates are weak bases in aqueous solution and typically ionize to form  $\text{NO}_3^-$ ; however, the basicity of the  $\text{NO}_3$  moiety can be higher than that of  $\text{H}_2\text{O}$  in nonaqueous media. For example, in strong acids such as neat nitric acid or concentrated sulfuric acid, protonation of nitric acid is a well-known source of nitronium ions  $\text{NO}_2^+$  and occurs by<sup>1</sup>



Upon dilution of the acid, the nitronium ion reacts with water to form  $\text{HNO}_3$  again.

Protonation of nitric acid has also been studied in the gas phase. Both theoretical and experimental studies have presented evidence for at least two structural isomers of protonated nitric acid consistent with the mechanisms in eqs 1a and 1b. Using a flowing afterglow apparatus, Fehsenfeld *et al.*<sup>2</sup> had first shown in 1975 that nitric acid protonated by  $\text{H}_3\text{O}^+$  behaved identically to  $\text{NO}_2^+(\text{H}_2\text{O})$ . In 1984, Nguyen and Hegarty,<sup>3</sup> using the self-consistent field (SCF) method with 4-31G and 6-31G\*\* basis sets, identified a variety of bound  $\text{H}_2\text{NO}_3^+$  isomers, but confirmed that the ion–molecule complex  $\text{NO}_2^+(\text{H}_2\text{O})$  is the most stable form. Cacace *et al.*,<sup>4</sup> performing metastable ion kinetic energy (MIKE) and collisionally induced dissociation (CID) spectrometry, confirmed the existence of two  $\text{H}_2\text{NO}_3^+$  structural isomers. Their results indicated that the more stable isomer contained a distinct  $\text{H}_2\text{O}$  moiety and that the less stable isomer released a significant amount of kinetic energy to give loss of  $\text{H}_2\text{O}$ . Finally, in 1992 Lee and Rice<sup>5</sup> revisited the computational characterization of protonated nitric acid, using levels of theory up to the coupled cluster method with triple excitations (CCSD(T)) and atomic natural orbital basis sets. They confirmed the previous experimental and theoretical studies, finding the covalently bound structural isomers of  $\text{H}_2\text{NO}_3^+$  (Figures 1b and 1c) to be at least 20 kcal/mol less stable than the  $\text{NO}_2^+(\text{H}_2\text{O})$  complex (Figure 1a).

The existence of more than one structural isomer has given rise to some ambiguity in the energetics. From a Fourier transform ion cyclotron resonance (FT-ICR) measurement, Cacace *et al.*<sup>4</sup> bracketed the gas phase proton affinity of  $\text{HNO}_3$  to  $168 \pm 3$  kcal/mol. This value was substantially lower than the proton affinity of 180 kcal/mol computed by Nguyen and Hegarty.<sup>3</sup> Subsequently, Lee and Rice<sup>5</sup> reported a proton affinity of  $182.5 \pm 4.0$  kcal/mol, leading to a binding energy for the  $\text{NO}_2^+(\text{H}_2\text{O})$  complex of  $D_0 = 17.3 \pm 2.0$  kcal/mol. In 1993, Sunderlin and Squires,<sup>6</sup> performing a CID experiment with a flowing afterglow triple quadrupole spectrometer, reported a dissociation energy of  $14.8 \pm 2.3$  kcal/mol and proton affinity of  $177.7 \pm 2.3$  kcal/mol. Subsequently, Cacace *et al.*<sup>7</sup> directly probed the relative proton affinities of nitric acid and methyl nitrate and found the proton affinity of  $\text{HNO}_3$  to be  $182.0 \pm$

<sup>†</sup> Present address: 313 Department of Chemistry, College of Science, Korea University, Anam-1-dong, Seongbuk-ku, Seoul, Korea 136-701.

<sup>‡</sup> Present address: Byk Gulden, Byk-Gulden-Strasse 2, D-78467, Konstanz, Germany.

<sup>⊗</sup> Abstract published in *Advance ACS Abstracts*, July 15, 1997.

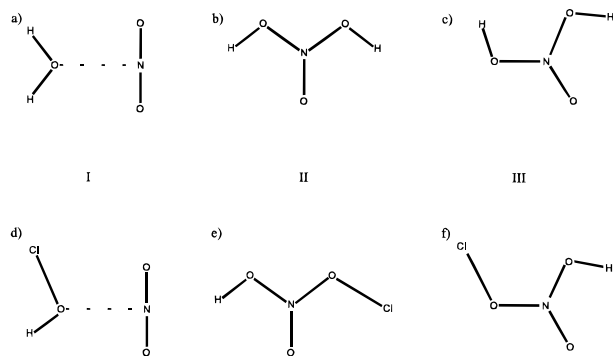


**Figure 1.** Structure of isomers of protonated nitric acid (a, b and c) and protonated chlorine nitrate (d, e, and f) obtained with correlated *ab initio* methods (refs 5 and 16). (I) The minimum energy isomers, the adducts  $\text{NO}_2^+(\text{H}_2\text{O})$  and  $\text{NO}_2^+(\text{HOCl})$ . (II) The W-shaped covalently bound isomers, which are about 20 kcal/mol above the ground state isomers. (III) The  $(\text{HO})_2\text{NO}^+$  isomer depicted (c) is the form that, without any internal rotations, can directly rearrange by a 1,3-hydrogen shift to give  $\text{NO}_2^+$  photoproducts. It is about 1 kcal/mol less stable than the W-shaped  $(\text{HO})_2\text{NO}^+$  isomer. The  $(\text{HO})(\text{ClO})\text{NO}^+$  isomer depicted (f) has an OH stretch frequency about  $15\text{ cm}^{-1}$  to the red of the W-shaped isomer's OH stretch. It is roughly 4 kcal/mol less stable than the W-shaped  $(\text{HO})(\text{ClO})\text{NO}^+$  isomer.

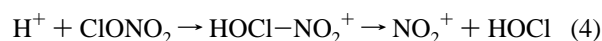
2.3 kcal/mol. Significantly, they attribute the ambiguity in their earlier bracketing measurement to the presence of the kinetically stable covalently bound isomer.

There has also been considerable recent interest in protonation reactions involving chlorine nitrate. The motivation has been to elucidate possible mechanisms for an important heterogeneous reaction occurring on Polar Stratospheric Clouds (PSCs):<sup>8–12</sup>



This reaction, which leads to the decomposition of a chlorine reservoir and releases active chlorine into the gas phase, is too slow to have been measured in the gas phase.<sup>13</sup> Molina and co-workers<sup>14</sup> proposed that the reaction might proceed by acid catalysis, because the surfaces of PSCs would be acidic due to the presence of  $\text{H}_2\text{SO}_4$ ,  $\text{HNO}_3$ , and  $\text{HCl}$ . This speculation has led to a number of studies on both the gas and condensed phase reactions of chlorine nitrate.

Among the gas phase studies, Nelson and Okumura<sup>15</sup> investigated the reaction of chlorine nitrate with small protonated water clusters,  $\text{H}_3\text{O}^+(\text{H}_2\text{O})_n$  ( $\langle n \rangle \approx 14$ ), in a relatively crude pick-up experiment and detected protonated nitric acid clusters,  $\text{NO}_2^+(\text{H}_2\text{O})_n$  ( $n = 0–2$ ), as reaction products. They proposed that protonation of chlorine nitrate led to formation of a weakly bound ion–molecule complex of  $\text{NO}_2^+$  and  $\text{HOCl}$



where the protonation occurs at the oxygen atom of the ClO group.

*Ab initio* calculations by Lee and Rice<sup>16</sup> confirmed the existence of this intermediate. They found that the lowest energy form of protonated chlorine nitrate is a complex of  $\text{NO}_2^+$  and  $\text{HOCl}$  (Figure 1d) bound by  $12.9 \pm 2$  kcal/mol at the CCSD-(T) level of correlation. They also found four other isomers formed by protonation of a terminal O atom (two of which are shown in Figures 1e and 1f), all with energies of approximately 20 kcal/mol or more above that of the ion–molecule complex. Similar results were obtained by Slanina *et al.*<sup>17</sup> at lower levels of theory.

In a more controlled selected-ion flow tube (SIFT) experiment, van Doren *et al.*<sup>18</sup> studied the thermal reaction of  $\text{H}_3\text{O}^+$

with  $\text{ClONO}_2$  and found this proton transfer reaction to be rapid ( $k = 2.9 \times 10^{-9}\text{ cm}^3\text{ s}^{-1}$  at 233 K). These authors directly observed  $\text{HClONO}_2^+$  (31% yield), although the primary product was  $\text{H}_2\text{NO}_3^+$ ;  $\text{NO}_2^+$  was a minor channel. These results were interpreted assuming protonated chlorine nitrate and protonated nitric acid to be adducts of  $\text{HOCl}$  and  $\text{H}_2\text{O}$  to  $\text{NO}_2^+$ . Chlorine nitrate was not found to react with small hydrated hydronium ions  $\text{H}_3\text{O}^+(\text{H}_2\text{O})_n$ ,  $n = 1–3$ .

Recently, Schindler *et al.*<sup>19</sup> examined the reactions of chlorine nitrate with a variety of hydrated ion clusters using a FT-ICR spectrometer. These elegant experiments have come the closest to using clusters to mimic aerosol chemistry. These authors found that distributions of clusters  $\text{H}_3\text{O}^+(\text{H}_2\text{O})_n$  peaked near  $n \approx 18$  reacted with chlorine nitrate to form predominantly  $\text{H}_3\text{O}^+(\text{H}_2\text{O})_m(\text{HNO}_3)$ . They attributed these products to direct reactions between chlorine nitrate and neutral  $\text{H}_2\text{O}$  in the solvation shells surrounding the ion. There was also a weak channel leading to formation of  $\text{NO}_2^+(\text{H}_2\text{O})_y$  with  $y = 0–2$ , similar to products detected by Nelson and Okumura,<sup>15</sup> which was assigned to rearrangement of small  $\text{H}_3\text{O}^+(\text{H}_2\text{O})_m(\text{HNO}_3)$  ( $m < 4$ ) clusters.

Spectroscopic studies can provide a direct measure of ion structure, complementing the existing mass spectrometric and kinetics experiments. Lee and co-workers pioneered the method of vibrational predissociation spectroscopy to obtain infrared spectra of mass-selected, weakly bound cluster ions.<sup>20</sup> Even low-resolution vibrational spectra in the X–H stretching region can be a sensitive probe of ion structure, particularly in conjunction with high level *ab initio* calculations. In some cases, such spectra were used to spectroscopically identify isomers.<sup>21</sup>

In previous work, we reported the infrared spectra of protonated nitric acid and higher hydrates in the  $2.6–3\text{ }\mu\text{m}$  wavelength region.<sup>22,23</sup> The spectrum of  $\text{H}_2\text{NO}_3^+$  was found to consist of two bands red-shifted by 31 and  $52\text{ cm}^{-1}$  from the symmetric and antisymmetric modes of  $\text{H}_2\text{O}$  monomer, respectively, in very good agreement with *ab initio* predictions. These results provided direct spectroscopic confirmation for the structure of protonated nitric acid as the adduct  $\text{NO}_2^+(\text{H}_2\text{O})$ .

In this paper, we used these methods to investigate the infrared spectroscopy of protonated  $\text{ClONO}_2$ ,  $\text{HNO}_3$ , and  $\text{DNO}_3$ . The use of different ionization sources allowed us to protonate these species under very different conditions. Comparison of the observed spectra with *ab initio* predictions of band positions calculated by Lee and Rice<sup>5,16</sup> allowed us to identify the absorbing species and distinguish among possible isomers.

## 2. Experiment

Spectra of ionic complexes were obtained by exciting mass-selected ions with an infrared laser and detecting the ionic photofragments from vibrational predissociation as a function of IR frequency. The experimental apparatus, a time-of-flight mass spectrometer and infrared optical parametric oscillator, has been described elsewhere.<sup>22–24</sup> In this section, only a brief description relevant to this experiment is presented.

Concentrated nitric acid (ca. 70% wt), deuterated nitric acid (68% in  $\text{D}_2\text{O}$ ), and  $\text{D}_2\text{O}$  were purchased from J.T. Baker Inc., Sigma Chemical Co., and Cambridge Isotope Lab. Inc., respectively. Ultrahigh purity (UHP) (99.999%) He and  $\text{H}_2$  were obtained from Matheson Gas Products Inc. Chlorine nitrate was synthesized from the reaction of  $\text{Cl}_2\text{O}$  with  $\text{N}_2\text{O}_5$ , following the procedure of Schmeisser.<sup>25</sup> The sample was purified using trap-to-trap distillation at 175 K to remove  $\text{Cl}_2$  and at 195 K to remove  $\text{Cl}_2\text{O}$ . Nitric acid impurities were excluded by transferring the  $\text{ClONO}_2$  through a cannula out of

the solid  $\text{HNO}_3$  at 195 K. Purified chlorine nitrate was a pale yellow solid at 77 K.

For the experiments with  $\text{HNO}_3$ , UHP  $\text{H}_2$  or He was seeded with  $\text{HNO}_3/\text{H}_2\text{O}$  vapor by passing the gas over a bubbler containing 70%  $\text{HNO}_3$  at 0 °C (partial pressures of  $p(\text{HNO}_3) = 0.79$  Torr and  $p(\text{H}_2\text{O}) = 1.1$  Torr).<sup>26</sup> The mixture of  $\text{HNO}_3$ ,  $\text{H}_2\text{O}$ , and  $\text{H}_2$  (or He) at a total stagnation pressure of 1000 Torr was pulsed into the vacuum (gas pulse width ca. 200  $\mu\text{s}$ ) through the 0.5-mm nozzle of a piezo-driven pulsed valve at a repetition rate of 10 Hz. The piezoelectric disc element was coated with halocarbon grease to prevent reactions with nitric acid occurring on the disc surface. Experiments on  $\text{DNO}_3$  were performed under similar conditions, with buffer gas passed over 70%  $\text{DNO}_3$  in  $\text{D}_2\text{O}$  at 0 °C.

Protonated  $\text{HNO}_3$  and  $\text{DNO}_3$  were produced in pulsed supersonic expansions by both glow discharge and electron-beam ionization sources. In the case of the electron beam source, a continuous electron beam (electron energy 750 eV) crossed the gas leaving the pulsed valve nozzle near the throat of the supersonic expansion. Typical emission and electron beam currents were  $\approx 2$  mA and 50–200  $\mu\text{A}$ , respectively. For the glow discharge source, the gas mixture was pulsed into a channel 1 mm in diameter and 1.5 cm in length. A high-voltage pulse (–1.5 to –3 kV, pulse width 100  $\mu\text{s}$ ) was applied between two electrodes near the channel entrance to initiate a glow discharge. The ions formed in the discharge source were thermalized as the gas flowed through the channel and further cooled in the supersonic expansion.

Protonated chlorine nitrate was generated in much the same way. However, due to its low boiling point and facile decomposition, extra care was taken in sample preparation. The chlorine nitrate was stored in an evacuated flask kept in liquid nitrogen (77 K) when not in use. To prepare the ion source, the gas inlet line was first evacuated and then passivated with chlorine nitrate by opening the sample flask and warming the sample in a dry ice bath (200 K) until the line pressure reached ca. 10 Torr, as measured by an MKS capacitance manometer. After the flask was closed, the gas line was passivated with  $\text{ClONO}_2$  for several hours. This was repeated several times. During the experiment, the  $\text{ClONO}_2$  sample was kept in a dry ice/acetone bath (195 K,  $p(\text{ClONO}_2) \approx 1$  Torr).<sup>27</sup>

In all experiments, the expanding plasma was skimmed and entered a time-of-flight chamber where the ions were extracted by a pulsed electric field (15  $\mu\text{s}$  pulse width) which accelerated the ions to 2.6 keV down a 2 m flight tube. A mass gate selected ions of a specific  $m/e$  and rejected all ions of other  $m/e$ . A pulsed tunable infrared laser, a  $\text{LiNbO}_3$  optical parametric oscillator with 1.5  $\text{cm}^{-1}$  resolution and 2–4 mJ of idler energy, was timed to excite the selected ions. Any ionic products formed from dissociation of parent ions excited by infrared radiation were separated from the parent ions using a reflectron energy analyzer and then detected by a microchannel plate detector. Action spectra were obtained by measuring the photofragment ion intensity as a function of the laser wavelength. Photofragment spectra were corrected by subtracting the background ion signal, primarily caused by dissociation of metastable parents in the ion optics chamber, and then normalizing to the laser fluence.

In experiments on protonated  $\text{DNO}_3$  and chlorine nitrate, the resolution of the time-of-flight mass spectra was carefully examined to confirm that the hydrogen and chlorine isotopomers were completely separated. In generating the  $\text{HDNO}_3^+$  ion ( $m/e = 65$ ),  $\text{H}_2\text{NO}_3^+$  and  $\text{D}_2\text{NO}_3^+$  ions ( $m/e = 64$  and 66, respectively) were also present. With a reflectron voltage  $V_{\text{REFL}} = +2650$  V and detector voltage  $V_{\text{DET}} = -1200$  V, each of

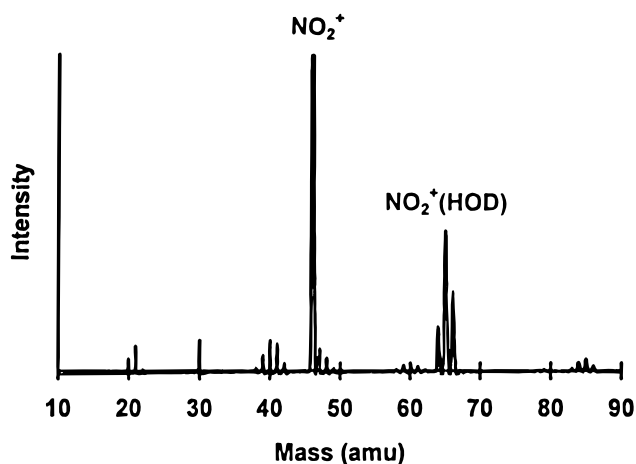


**Figure 2.** Time-of-flight mass spectrum of the protonated  $\text{DNO}_3$  hydrate ion  $\text{NO}_2^+(\text{HOD})$  ( $m/e = 65$ ) formed by electron beam ionization of  $\text{DNO}_3/\text{D}_2\text{O}$  vapor from 70%  $\text{DNO}_3$  seeded in  $\text{H}_2$ .

these peaks had a typical full-width-at-half-maximum (FWHM) of 100 ns, and the peak-to-peak separation between two neighboring peaks (i.e., either  $m/e = 64$  and 65, or 65 and 66) was 270 ns. This separation was sufficient to allow the mass gate to effect mass selection.

However, at the higher detector voltages required to observe the photofragmentation of  $\text{HDNO}_3^+$ , background peaks were observed. This small background signal arose from fragmentation of a small fraction of metastable  $\text{H}_2\text{NO}_3^+$  and  $\text{D}_2\text{NO}_3^+$  parent ions present in the detector region. With the reflectron voltage lowered to  $(m_i/m_p)V_{\text{REFL}}$ , the arrival times of the unwanted metastable decay products were shifted closer to the arrival time of the photofragments. If the resolution were too low, metastables and photofragments would partially overlap. To check this possibility, the time profiles of photoproducts together with those of neighboring metastable fragment ions were carefully monitored at a much higher detector voltage,  $V_{\text{DET}} = -1700$  V. In the case of  $\text{HDNO}_3^+$  photodissociation, the FWHM of both the  $\text{H}_2\text{NO}_3^+$  and  $\text{D}_2\text{NO}_3^+$  metastable peaks were about 60 ns. When  $V_{\text{REFL}}$  was changed from +2650 to +1875 V, the difference in flight times of photofragments and neighboring metastables was about 100 ns. Since our integration range for the photofragment peak was about 80 ns wide, contamination of photofragment signals by unwanted neighboring metastable ions was negligible.

### 3. Experimental Results

Typical time-of-flight mass spectra of the protonated  $\text{DNO}_3$  and  $\text{ClONO}_2$  species are shown in Figures 2 and 3. Mass spectra of protonated  $\text{HNO}_3$  and higher hydrate clusters,  $\text{NO}_2^+(\text{H}_2\text{O})_n$  ( $n = 0-5$ ), formed in a pulsed discharge source have been reported previously.<sup>22,23</sup> Figure 2 shows protonated  $\text{DNO}_3$  hydrate clusters formed by electron beam ionization.  $\text{NO}_2^+(\text{H}_2\text{O})$ ,  $\text{NO}_2^+(\text{HOD})$ , and  $\text{NO}_2^+(\text{D}_2\text{O})$  ( $m/e = 64, 65$ , and 66, respectively) are well resolved. Mass spectra obtained by ionizing gas mixtures containing chlorine nitrate are shown in Figure 3. Protonated chlorine nitrate could be observed upon electron beam ionization (Figure 3a), but not when ionized in the glow discharge source (Figure 3b). The natural relative abundances of  $^{35}\text{Cl}$  and  $^{37}\text{Cl}$  are reflected in the mass spectrum of  $\text{HClONO}_2^+$ , with the peaks at  $m/e = 98$  and 100 having a 3:1 intensity ratio.

We recorded infrared spectra of protonated  $\text{HNO}_3$ ,  $\text{DNO}_3$ , and  $\text{ClONO}_2$  in the 3300–3750  $\text{cm}^{-1}$  region. Figures 4–6 present the infrared spectra for the protonated ion species over this frequency range, and Table 1 lists the observed maxima.

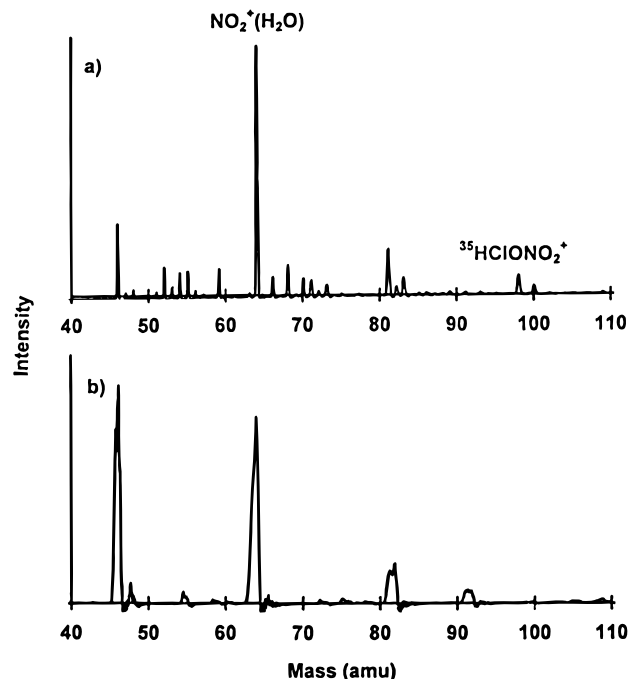


**Figure 3.** Time-of-flight mass spectra of chlorine nitrate seeded in  $\text{H}_2$ , ionized (a) by an electron beam and (b) in a glow discharge. Protonated chlorine nitrate,  $\text{HClONO}_2^+$ , is seen only in spectrum a. The two chlorine isotopomers can be seen at  $m/e = 98$  and 100.

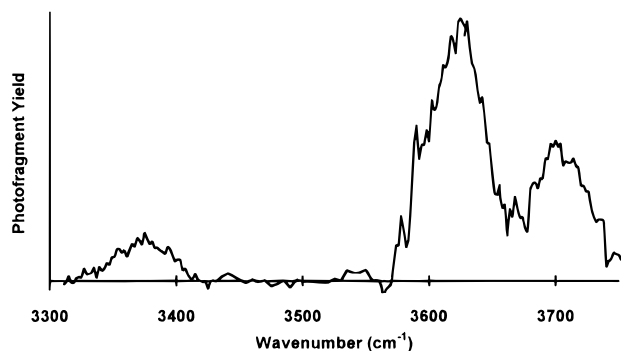


**Figure 4.** Vibrational predissociation spectrum of protonated nitric acid formed by electron beam ionization of the free jet expansion.

**A. Photodissociation Behavior.**  $\text{NO}_2^+$  was the only photofragment ion detected upon infrared excitation of all of the protonated species studied here, indicating that the only dissociation channel was

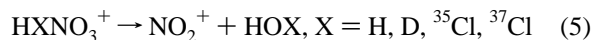
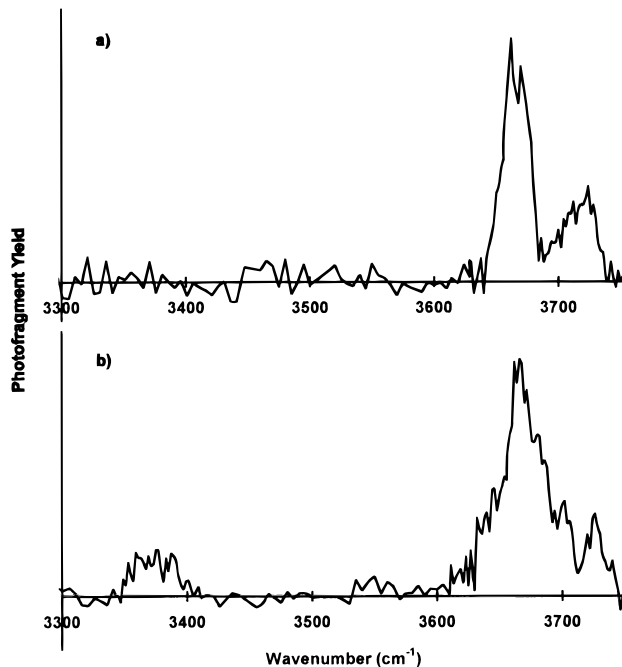
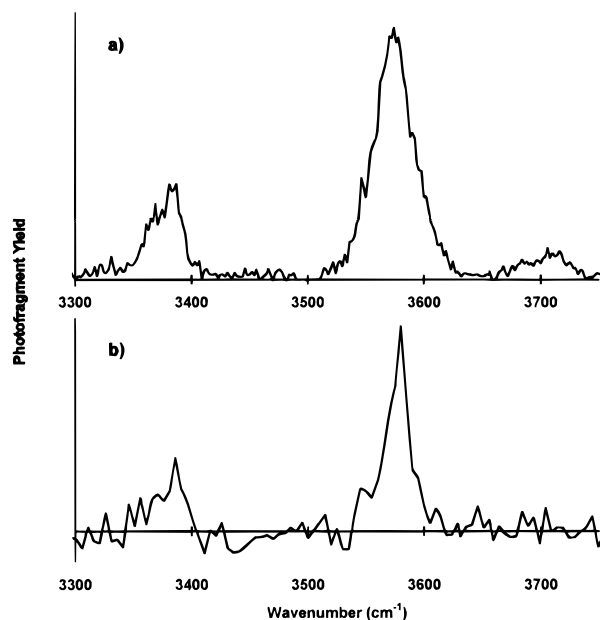


Figure 7 shows the dependence of the photodissociation signal on OPO idler energy for protonated nitric acid and chlorine nitrate with the laser frequency set to the maximum of their respective photofragment spectra. For  $\text{NO}_2^+(\text{H}_2\text{O})$  formed by the glow discharge source, the  $3626 \text{ cm}^{-1}$  band showed a nearly quadratic dependence (Figure 7a). For the  $\text{NO}_2^+(\text{HO}^{35}\text{Cl})$  from electron beam ionization, the  $3574 \text{ cm}^{-1}$  band possessed a nearly linear dependence (Figure 7b). In both cases, a sum of linear and quadratic terms gave a better fit to the power dependence curve than either term alone, although one term dominated in each case. Similar behavior has been observed in other cluster studies, e.g., the photodissociation of  $\text{NO}^+(\text{H}_2\text{O})_n$  ions.<sup>24</sup>

**B. Vibrational Predissociation Spectra.** The infrared spectrum of protonated nitric acid depended upon the method of ion generation. As reported previously,<sup>22,23</sup> the spectrum of



**Figure 5.** Vibrational predissociation spectra of  $\text{HDNO}_3^+$  formed (a) in a glow discharge and (b) by electron beam ionization of the free jet expansion.



**Figure 6.** Vibrational predissociation spectra of the two isotopomers of protonated chlorine nitrate,  $\text{HClONO}_2^+$ , formed by electron beam ionization of the free jet expansion. Spectra were recorded for parent ions of (a)  $m/e = 98$  and (b)  $m/e = 100$ .

$\text{H}_2\text{NO}_3^+$  formed in the glow discharge source possessed two absorption bands in the  $3300\text{--}3750 \text{ cm}^{-1}$  region. The lower frequency band, with partially resolved  $P$ ,  $Q$ , and  $R$  sub-bands, was centered at  $3626 \text{ cm}^{-1}$ . The second band, centered at  $3704 \text{ cm}^{-1}$ , was a doublet with maxima at  $3700$  and  $3708 \text{ cm}^{-1}$ . When  $\text{H}_2\text{NO}_3^+$  was formed by the electron beam ionization source, an additional broad, featureless band appeared at  $3375 \text{ cm}^{-1}$  (Figure 4). Furthermore, the two bands in the  $3600\text{--}3750 \text{ cm}^{-1}$  region were broader than those observed with the discharge source.

The infrared spectrum of protonated  $\text{DNO}_3$  ion also differed depending on the source, as shown in Figure 5. The spectrum of  $\text{HDNO}_3^+$  ions generated in the discharge source (Figure 5a) possessed two bands, a strong band centered at  $3666 \text{ cm}^{-1}$  and

TABLE 1: Vibrational Frequencies of Protonated HNO<sub>3</sub> and Protonated ClONO<sub>2</sub>

protonated species	frequency/cm <sup>-1</sup>			assignment
	discharge source	electron beam source	scaled <i>ab initio</i> <sup>a</sup>	
NO <sub>2</sub> <sup>+</sup> (H <sub>2</sub> O)	3626 <sup>j</sup>	3625	3607 <sup>b</sup>	H <sub>2</sub> O symmetric stretch
	3700, 3708 <sup>j</sup>	3698	3701 <sup>b</sup>	H <sub>2</sub> O antisymmetric stretch
(HO) <sub>2</sub> NO <sup>+</sup>		3375	3393 <sup>c</sup>	OH stretch
NO <sub>2</sub> <sup>+</sup> (HOD)	3666	3666	3683 <sup>d</sup>	OH stretch
	3724	3726	3747 <sup>e</sup>	NO <sub>2</sub> <sup>+</sup> ν <sub>1</sub> + ν <sub>3</sub> combination band
(HO)(DO)NO <sup>+</sup>		3380		OH stretch
NO <sub>2</sub> <sup>+</sup> (HO <sup>35</sup> Cl)		3574	3582 <sup>f</sup>	OH stretch
		3706	3731 <sup>e</sup>	NO <sub>2</sub> <sup>+</sup> ν <sub>1</sub> + ν <sub>3</sub> combination band
(HO)( <sup>35</sup> ClO)NO <sup>+</sup>		3369, 3384	3397, 3413 <sup>g</sup>	OH stretch
NO <sub>2</sub> <sup>+</sup> (HO <sup>37</sup> Cl)		3580	3582 <sup>h</sup>	OH stretch
(HO)( <sup>37</sup> ClO)NO <sup>+</sup>		3386	3394 <sup>i</sup>	OH stretch

<sup>a</sup> Taken from refs 5, 16, and 29. <sup>b</sup> The MP2/TZ2P value was scaled by the average of the experimental stretches of H<sub>2</sub>O. <sup>c</sup> The MP2/DZP value for the stronger band of isomer II was scaled by the experimental OH stretch of HNO<sub>3</sub>. <sup>d</sup> The CCSD(T)/DZP value was scaled by the average of the experimental stretches of H<sub>2</sub>O and then corrected for the isotope shift. <sup>e</sup> The CCSD(T)/DZP value was scaled by the experimental (matrix) value for NO<sub>2</sub><sup>+</sup>; the isotopic shift was <1 cm<sup>-1</sup>. <sup>f</sup> The MP2/TZ2P value was scaled by the experimental OH stretch of HOCl. <sup>g</sup> The MP2/DZP values of isomers II and III were scaled by the experimental OH stretch of HOCl. <sup>h</sup> The MP2/TZ2P value was scaled by the experimental OH stretch of HOCl; the isotopic shift was <1 cm<sup>-1</sup>. <sup>i</sup> The MP2/TZ2P value for the W-shaped isomer (II) was scaled by the experimental OH stretch of HOCl; the isotopic shift was <1 cm<sup>-1</sup>. <sup>j</sup> Taken from refs 22 and 23.

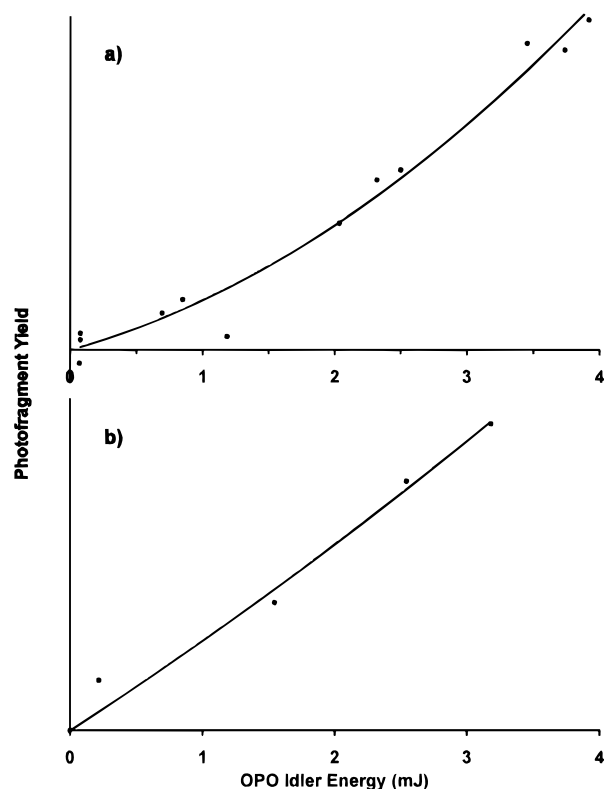


**Figure 7.** Dependence on laser pulse energy of the fragment signal from photodissociation of the parent ions (a) NO<sub>2</sub><sup>+</sup>(H<sub>2</sub>O) at 3626 cm<sup>-1</sup> and (b) NO<sub>2</sub><sup>+</sup>(HO<sup>35</sup>Cl) at 3574 cm<sup>-1</sup>. The data in both (a) and (b) are fit by a sum of linear and quadratic terms. The fits indicate a nearly quadratic power dependence for NO<sub>2</sub><sup>+</sup>(H<sub>2</sub>O) and a nearly linear power dependence for NO<sub>2</sub><sup>+</sup>(HO<sup>35</sup>Cl).

a weaker satellite at 3724 cm<sup>-1</sup>, while the spectrum of ions formed by electron beam ionization in the jet (Figure 5b) exhibited an additional band at 3380 cm<sup>-1</sup>.

Protonated chlorine nitrate was produced only by electron beam ionization. The infrared spectrum of H<sup>35</sup>ClONO<sub>2</sub><sup>+</sup>, shown in Figure 6a, consisted of three bands. The strongest band was centered at 3574 cm<sup>-1</sup>, accompanied by a weak band at 3706 cm<sup>-1</sup>. In addition, there was an absorption of medium intensity centered at 3377 cm<sup>-1</sup> which possibly contained sub-bands at 3369 and 3384 cm<sup>-1</sup>. Similar features appeared in the spectrum (Figure 6b) of the <sup>37</sup>Cl isotopomer, although the weak band was not observed due to the poor signal-to-noise ratio.

## 4. Discussion

### A. Vibrational Spectra of Protonated HNO<sub>3</sub> and DNO<sub>3</sub>

We have previously reported<sup>22,23</sup> infrared spectra of protonated nitric acid which demonstrated that H<sub>2</sub>NO<sub>3</sub><sup>+</sup> (produced in a glow discharge source) is an ion–molecule complex NO<sub>2</sub><sup>+</sup>(H<sub>2</sub>O) (Figure 1a) undergoing vibrational predissociation to NO<sub>2</sub><sup>+</sup> and H<sub>2</sub>O. The observed infrared spectrum of NO<sub>2</sub><sup>+</sup>(H<sub>2</sub>O) is analogous to that of a water molecule. The two bands at 3626 and 3704 cm<sup>-1</sup> were assigned to the symmetric and antisymmetric stretches of the H<sub>2</sub>O ligand, red-shifted by 31 and 52 cm<sup>-1</sup>, respectively, due to perturbation by the NO<sub>2</sub><sup>+</sup> ion core. These band positions agreed well with vibrational frequencies (scaled to the experimental frequencies of H<sub>2</sub>O) computed by Lee and Rice at the second-order Møller–Plesset (MP2) level with a triple-ζ basis set.<sup>5</sup> The nearly quadratic fluence dependence of the photodissociation allows us to bracket the adduct binding energy between 10.5 and 21 kcal/mol, consistent with previous experimental and theoretical estimates of the cluster dissociation energy.<sup>5–7</sup>

The current results on protonated DNO<sub>3</sub> formed in the glow discharge source agree with the earlier experiments. The spectrum of HDNO<sub>3</sub><sup>+</sup> formed in the discharge source (Figure 5a) can similarly be attributed to that of a NO<sub>2</sub><sup>+</sup>(HOD) complex. The strongest band at 3666 cm<sup>-1</sup> is red-shifted by only 41 cm<sup>-1</sup> from the OH stretch of free HOD.<sup>28</sup> Moreover, using their CCSD(T)/DZP force field for NO<sub>2</sub><sup>+</sup>(H<sub>2</sub>O), Lee and Rice<sup>29</sup> predict a (scaled) OH stretch of 3683 cm<sup>-1</sup>. We therefore assign the 3666 cm<sup>-1</sup> band to the OH stretch of the perturbed HOD bound to NO<sub>2</sub><sup>+</sup>.

We would expect this OH stretch to be the only vibration of NO<sub>2</sub><sup>+</sup>(HOD) observed above 3000 cm<sup>-1</sup>. The observation of a second band of HDNO<sub>3</sub><sup>+</sup> at 3724 cm<sup>-1</sup> is therefore surprising. We can rule out contamination from the adjacent (in the time-of-flight domain) undeuterated parent ion NO<sub>2</sub><sup>+</sup>(H<sub>2</sub>O), because no fragmentation was observed upon excitation at 3626 cm<sup>-1</sup>, one of the two strong peaks of NO<sub>2</sub><sup>+</sup>(H<sub>2</sub>O). The 3724 cm<sup>-1</sup> band is also unlikely to be a combination band of the OH stretch with a lower frequency mode of the cluster. The intermolecular N=O stretch of NO<sub>2</sub><sup>+</sup>(HOD) is predicted<sup>5,29</sup> to be 224 cm<sup>-1</sup>, which would place a combination band of the OH stretch and N=O stretch at 3890 cm<sup>-1</sup>.

One alternative is to assign the 3724-cm<sup>-1</sup> band to a vibrational transition of the NO<sub>2</sub><sup>+</sup> ion. Forney *et al.*<sup>30</sup> have reported a similar band in the IR spectra of NO<sub>2</sub><sup>+</sup> trapped in rare gas matrices. They observed a transition at 3711 cm<sup>-1</sup> in

a neon matrix which they assigned to the combination of the symmetric and antisymmetric stretch modes,  $\nu_1 + \nu_3$ , of  $\text{NO}_2^+$ . This vibration is likely to be only weakly perturbed in the matrix and hence will be close to the gas phase value. Lee and Rice<sup>5</sup> have also found that the fundamental frequencies of  $\text{NO}_2^+$  will also be shifted only slightly upon binding  $\text{H}_2\text{O}$ . Their *ab initio* calculations on  $\text{NO}_2^+$  and  $\text{NO}_2^+(\text{H}_2\text{O})$  at identical levels of theory predict that the harmonic frequencies of  $\nu_1 + \nu_3$  will change upon forming the complex by only +36 or +44  $\text{cm}^{-1}$  at the CCSD(T)/DZP and MP2/TZ2P levels, respectively. We therefore assign the 3724  $\text{cm}^{-1}$  band to the  $\nu_1 + \nu_3$  combination band of the  $\text{NO}_2^+$  ion core.

The 3724  $\text{cm}^{-1}$  band is relatively intense for a combination band, and the intensity may be enhanced through a Fermi resonance with the nearby OH stretch. This combination band should also be present for  $\text{NO}_2^+(\text{H}_2\text{O})$  but would then be mixed with the strong antisymmetric stretch band of the  $\text{H}_2\text{O}$  ligand, which appears at 3704  $\text{cm}^{-1}$ . We searched for this band in the  $\text{NO}_2^+(\text{D}_2\text{O})$  system as well, but we did not observe any photofragmentation bands in the 3700  $\text{cm}^{-1}$  region. If the assignment to the  $\text{NO}_2^+$  combination band is correct, then the absence of signal could be interpreted as a lack of intensity enhancement through a Fermi resonance, since there are no other bands nearby. This negative result does, however, leave open the possibility that our assignment is incorrect; the most plausible alternative is to assign the 3724  $\text{cm}^{-1}$  band to a combination band of a low-frequency intermolecular mode with the OH stretch. However, the observation of a similar band in  $\text{NO}_2^+(\text{HOCl})$  at a nearly identical frequency (see below) provides further evidence in support of our assignment to the  $\text{NO}_2^+$  intramolecular combination band.

A new band near 3375  $\text{cm}^{-1}$  is observed in the spectrum of protonated  $\text{HNO}_3$  when these ions are generated by the electron beam source (Figure 4). A nearly identical band also appears (at 3380  $\text{cm}^{-1}$ ) in the spectrum of protonated  $\text{DNO}_3$  formed with the same source (Figure 5b). The appearance of these bands under one set of source conditions indicates that they should be assigned to new isomers of protonated  $\text{HNO}_3$  and protonated  $\text{DNO}_3$ . We assign these bands to the metastable isomers  $(\text{HO})_2\text{NO}^+$  and  $(\text{HO})(\text{DO})\text{NO}^+$ .

Lee and Rice<sup>5</sup> predict two related metastable  $(\text{HO})_2\text{NO}^+$  isomers. Both are planar and possess similar stabilities, differing primarily in the relative orientations of the two OH groups. Isomer II (Figure 1b) is predicted to possess a very strong band (MP2/DZP scaled) at 3393  $\text{cm}^{-1}$  and one weak band at 3406  $\text{cm}^{-1}$ . Isomer III (Figure 1c) is predicted to possess strong bands at 3392 and 3410  $\text{cm}^{-1}$ . In our spectra (Figures 4 and 5b), we did not resolve any definitive structure within the 3375  $\text{cm}^{-1}$  band. Therefore, we cannot determine from the IR spectra if one, or a mixture, of the metastable isomers was present in the beam. However, it is the case that the strongest absorption predicted, the one at 3393  $\text{cm}^{-1}$  (622 km/mol), is within 18  $\text{cm}^{-1}$  of the observed band center. Our spectra, then, do unambiguously show the presence of metastable isomers formed by protonation of one of the terminal O atoms.

Observation of different spectra from the two types of ion sources can be rationalized in terms of the extent of collisional relaxation. Both ion–molecule adducts and metastable isomers are likely to be formed upon direct protonation of nitric acid. In the discharge source, a high-pressure plasma occurs in a narrow channel just after the valve orifice. The ions undergo  $10^3$  or more thermalizing collisions as the gas flows through the channel and are further cooled in the ensuing supersonic expansion. Higher energy isomers formed in the discharge will then undergo enough collisions to rearrange and dissociate,

forming adducts during subsequent clustering. The ion beam would then contain only the lowest energy ion–molecule complex. In the electron beam source, however, the plasma is generated somewhat downstream of the throat of the expansion. Ions formed will undergo significantly fewer collisions; it is therefore plausible that some metastable isomers formed by initial protonation of a terminal O atom remain.

**B. Vibrational Spectrum of Protonated  $^{35,37}\text{ClONO}_2$ .** The spectrum of protonated chlorine nitrate generated by the electron beam source (Figure 6a) is composed of three bands with a pattern similar to the spectrum of  $\text{HDNO}_3^+$  formed by the same method. The similarity of the spectrum for the parent ion at  $m/e = 100$  (Figure 6b), the  $^{37}\text{Cl}$  isotopomer, confirms the assignment of this spectrum to  $\text{HClONO}_2^+$ . The spectrum can be assigned in an analogous manner.

We assign the two bands in the 3500–3750  $\text{cm}^{-1}$  region to excitation of vibrations of the weakly bound ion–molecule complex  $\text{NO}_2^+(\text{HOCl})$ . The strongest band at 3574  $\text{cm}^{-1}$  is red-shifted by only 35  $\text{cm}^{-1}$  from the OH stretch of  $\text{HOCl}$  monomer<sup>31</sup> and is assigned to the OH stretch of the  $\text{HOCl}$  ligand. The weak band at 3706  $\text{cm}^{-1}$ , which possesses approximately one-fifth of the intensity of the OH stretch, is clearly analogous to the 3724  $\text{cm}^{-1}$  band of  $\text{NO}_2^+(\text{HOD})$ ; we attribute this transition to the same combination of symmetric and antisymmetric stretches of the  $\text{NO}_2^+$  ion core. This band appears at nearly the same frequency for the two complexes, despite the large difference in OH stretch frequencies. This fact argues strongly for the current assignment, rather than a combination band involving the OH stretch and an intermolecular mode, which for  $\text{NO}_2^+(\text{HOCl})$  would result in the higher frequency mode's red-shifting almost 100  $\text{cm}^{-1}$  with the OH stretch.

Finally, we assign the medium intensity band centered at 3377  $\text{cm}^{-1}$  to the OH stretch of the metastable isomer(s)  $(\text{HO})(\text{ClO})\text{NO}^+$ , in analogy to our assignment of the 3375  $\text{cm}^{-1}$  bands observed in the spectra of both protonated  $\text{H}_2\text{NO}_3^+$  and  $\text{HDNO}_3^+$ . Our assignment of this band to a different isomer of  $\text{HClONO}_2^+$  is somewhat less firm, since we are unable to compare spectra taken with different sources. However, the similarity with protonated nitric acid is highly suggestive. Our hypothesis of a second isomer implies that the electron-beam-generated ion beam contains a mixture of isomers, as in the case of protonated nitric acid.

The observed bands in the infrared spectrum agree quite well with *ab initio* vibrational frequencies.<sup>16</sup> The calculations predict that the lowest energy form of protonated  $\text{ClONO}_2$  corresponds to a complex between  $\text{HOCl}$  and  $\text{NO}_2^+$  (Figure 1d), similar to the case for nitric acid. The (scaled) *ab initio* OH stretch of  $\text{NO}_2^+(\text{HOCl})$ , 3582  $\text{cm}^{-1}$ , agrees very well with the band at 3574  $\text{cm}^{-1}$ .

Unlike the analogous features in the protonated nitric acid spectra (Figures 4 and 5b), the band centered at 3377  $\text{cm}^{-1}$  (Figure 6a) appears to have some structure, with maxima separated by around 15  $\text{cm}^{-1}$ . Interestingly, two of the metastable isomers of  $(\text{HO})(\text{ClO})\text{NO}^+$  found by Lee and Rice,<sup>16</sup> labeled as II and III in Figure 1, are predicted to have (scaled) OH stretch frequencies (3413 and 3397  $\text{cm}^{-1}$ , respectively) that also differ by around 15  $\text{cm}^{-1}$ . Isomer II, the so-called “W-shaped isomer”, is roughly 20 kcal/mol less stable than the ion–molecule complex, and isomer III, in turn, is roughly 4 kcal/mol less stable than the W-shaped isomer.

Of course, the signal-to-noise ratio of the 3377  $\text{cm}^{-1}$  feature is not high enough to say with certainty that the apparent structure is real, but if it is, this would constitute spectroscopic evidence for the presence of at least two different covalently bound isomers. Qualitatively, a measurable difference in OH

stretch frequency is not unreasonable, in that in isomer II the protonated O atom is *trans* to the Cl, whereas in isomer III the protonated O atom is *cis* to the Cl.

In any case, however, the absorption centered at  $3377\text{ cm}^{-1}$  is no more than  $40\text{ cm}^{-1}$  from the (scaled) OH stretch frequencies predicted by Lee and Rice for three of the four covalently bound  $(\text{HO})(\text{ClO})\text{NO}^+$  isomers they identified.<sup>16</sup> This, coupled with the lack of many thermalizing collisions in the electron beam source that generated the protonated chlorine nitrate, strongly suggests that the ion beam contained at least one  $\text{HClONO}_2^+$  isomer besides the ion-molecule complex  $\text{NO}_2^+(\text{HOCl})$ .

The measurement of photofragment signal at  $3574\text{ cm}^{-1}$  as a function of laser fluence (Figure 7b) shows that the dependence is nearly linear, indicating that only one photon is required to dissociate the protonated species. This observation suggests that the binding energy of protonated chlorine nitrate is smaller than that of protonated nitric acid and closer to the photon energy of ca.  $10.2\text{ kcal/mol}$ . This limit is consistent with the *ab initio* value of  $12.9 \pm 2.0\text{ kcal/mol}$  at the CCSD(T) level of theory.<sup>16</sup>

In contrast to the electron beam ionization method, no protonated chlorine nitrate was found to be produced in the glow discharge (Figure 3b). This fact can be ascribed to the likelihood of switching reactions, given the large number of collisions occurring in the discharge source. Replacement of HOCl by  $\text{H}_2\text{O}$  is thermodynamically favored, because the proton affinity of chlorine nitrate is lower than that of nitric acid. This is clear from the study of van Doren *et al.*,<sup>18</sup> who have shown that under thermal conditions ( $233\text{ K}$ ) collisions between  $\text{H}_3\text{O}^+$  and  $\text{ClONO}_2$  are twice as likely to form  $\text{NO}_2^+(\text{H}_2\text{O})$  as  $\text{NO}_2^+(\text{HOCl})$ .

### C. Evidence for Isomerization Induced by IR Excitation.

The observation of vibrational predissociation spectra of the  $(\text{HO})_2\text{NO}^+$  and  $(\text{HO})(\text{ClO})\text{NO}^+$  isomers is unexpected, because these isomers are covalently bound. Unlike the ground state, the metastable isomers are not ion-molecule adducts, and the two H atoms (or H and Cl atoms) are bound to different O atoms. Dissociation to  $\text{NO}_2^+ + \text{HOX}$  products can therefore only occur if these metastable isomers undergo an intramolecular rearrangement, as shown in Figure 8. Specifically, upon absorbing one or at most two infrared photons, intramolecular hydrogen atom transfer must occur by a 1,3 hydrogen shift from one hydroxyl to the other to form an  $\text{H}_2\text{O}$  (or HOCl) moiety. This transfer will be accompanied by a simultaneous weakening of the  $\text{XHO}\cdots\text{N}$  bond and transfer of charge from the protons to the nitrogen atom. The extent of charge transfer may in fact be relatively small, because the N atom and both H atoms already possess significant positive charge (on the order of  $+0.5$  or greater). The result of the isomerization is formation of the  $\text{NO}_2^+(\text{HOX})$  adduct with internal energies well above the complex dissociation limit. Because the initial N-O bond length is significantly shorter in the covalent isomer, the fragments are likely to dissociate promptly once over the barrier with a large fraction of available energy partitioned into fragment translation.

An energy level diagram for protonated nitric acid and protonated chlorine nitrate is given in Figure 8, where we have grouped together the two sets of isomers into covalently bound metastables and ground state adducts since these cannot be distinguished in this experiment. The energetics are roughly comparable, with the metastable species lying approximately  $20\text{ kcal/mol}$  above the adduct energy for both systems.

For protonated nitric acid, our results suggest that the barrier for H atom transfer and simultaneous charge transfer is on the

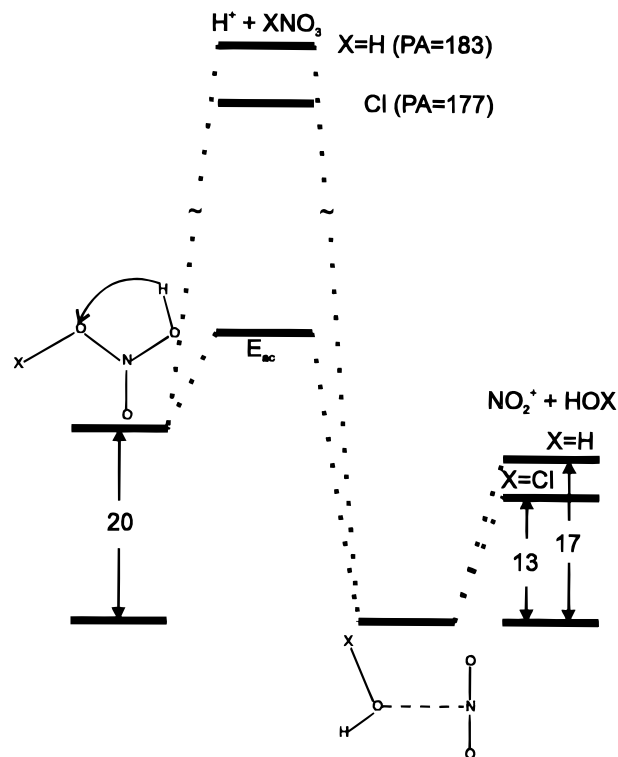


**Figure 8.** Energy level diagram for the protonation reaction of  $\text{HNO}_3$  and  $\text{ClONO}_2$ . Energies used in this diagram are the *ab initio* values computed by Lee and Rice (refs 5 and 16). The activation energy for isomerization is unknown.

order of  $9.7\text{ kcal/mol}$ , the energy of one  $3375\text{ cm}^{-1}$  photon. Because the ions may be hot, we cannot exclude the possibility that the activation energy is greater than this value and that only a fraction of ions possess sufficient internal energy to dissociate upon absorbing a single photon.

The current results are qualitatively consistent with the observations of Cacace *et al.*<sup>4</sup> on two isomers of protonated nitric acid. In MIKE (metastable ion kinetic energy release) experiments, these authors found one isomer which dissociated with little energy release and assigned this to the  $\text{NO}_2^+(\text{H}_2\text{O})$  adduct structure. They identified a second isomer, formed by more exothermic proton transfer, which released considerable kinetic energy upon dissociation. They set a lower limit of  $21\text{ kcal/mol}$  for the barrier height relative to dissociated products. The magnitude of the translational energy release observed by Cacace *et al.*<sup>4</sup> is somewhat higher than one expects, given the results of our experiment and the *ab initio* calculations of Lee and Rice.<sup>5</sup> The theory indicates that the covalent isomers lie  $21\text{ kcal/mol}$  above the minimum energy adduct isomer and  $4\text{ kcal/mol}$  above the dissociation limit. Our upper limit of  $9.7\text{ kcal/mol}$  for dissociation of the covalent isomer leads to a barrier  $14\text{ kcal/mol}$  above the dissociation limit,  $7\text{ kcal/mol}$  below Cacace's lower limit. This discrepancy can be accounted for by one or more of the following possibilities: (a) two photons are required to dissociate these complexes, leading to  $24\text{ kcal/mol}$  of available energy, (b) the covalent ions dissociated in our experiment possess  $6$  or more  $\text{kcal/mol}$  of internal energy, (c) the binding energy of  $\text{NO}_2^+(\text{H}_2\text{O})$  is closer to the lower value of  $14.8\text{ kcal/mol}$  observed by Sunderlin and Squires,<sup>6</sup> or (d) Cacace *et al.* are observing dissociation of isomer II (the W-shaped isomer), which may have to surmount an additional barrier for OH rotation to form isomer III which then subsequently dissociates by H atom transfer (Figure 1). The last process has been postulated by Lee and Rice, although no transition state energies have been calculated.

**D. Protonation Reactions of Chlorine Nitrate.** Our results provide direct spectroscopic evidence that protonation of chlorine nitrate leads to formation of both an adduct  $\text{NO}_2^+(\text{HOCl})$  and a metastable covalently bound isomer  $(\text{ClO})(\text{HO})\text{-NO}^+$ . According to the calculations of Lee and Rice,<sup>16</sup> the gas phase reaction



is exothermic by 11 kcal/mol to form the adduct  $\text{NO}_2^+(\text{HOCl})$ . These calculations indicate that formation of the metastable isomers would lead to a reaction enthalpy of at least  $\Delta H = +9$  kcal/mol; therefore, covalently bound isomers would be unobserved under thermal conditions. The electron beam ionization of a supersonic jet is a highly nonequilibrium plasma. The metastable isomers may be formed by a variety of methods including more exothermic protonation reactions, e.g., between chlorine nitrate and species such as  $\text{H}_3^+$ .

The current study is one of several investigating the gas phase protonation of chlorine nitrate. One motivation of these studies was to investigate whether gas phase mechanisms could shed light on possible mechanisms for the heterogeneous reaction of  $\text{ClONO}_2$  with  $\text{H}_2\text{O}$  on water ice and other stratospheric aerosols. In the gas phase, the reaction of  $\text{ClONO}_2$  results in the weakening of the N—O bond and formation of the  $\text{NO}_2^+(\text{HOCl})$  adduct, which had led to the suggestion<sup>15,16</sup> that  $\text{HOCl}$  could be formed by protonation of the  $\text{ClO}$  moiety. However, the cluster studies<sup>18,19</sup> now indicate that direct reaction of  $\text{H}_3\text{O}^+$  with  $\text{ClONO}_2$  does not occur in the presence of additional  $\text{H}_2\text{O}$ ; rather, the reactions occur only for larger clusters (as is the case for reactions of  $\text{H}_3\text{O}^+(\text{H}_2\text{O})_n$  with  $\text{HNO}_3$ <sup>32</sup>). A similar conclusion has been reached from recent bulk measurements with water ice, particularly the IR studies of Sodeau<sup>33</sup> and the elegant isotope studies of Hanson.<sup>34</sup>

Direct protonation of chlorine nitrate in the condensed phase is likely to be of importance only under nonaqueous or highly acidic conditions, similar to conditions leading to protonation of nitric acid. Under these conditions,  $\text{H}_3\text{O}^+$  stabilization by hydration is limited, the energetics become more comparable to the gas phase, and adduct formation may occur (as is the case for protonation of  $\text{HONO}$  and  $\text{HNO}_3$ ). There is some indication of a different mechanism operable in sulfuric acid;<sup>35,36</sup> however, it is not clear if background sulfuric acid aerosols (<70 wt %) are sufficiently acidic. In more concentrated sulfuric acid other reactions may become important, e.g., direct reaction with  $\text{H}_2\text{SO}_4$ . Further experiments, for example with detection of  $\text{NO}_2^+$ , are needed to establish if reaction 4 occurs in acidic conditions in the condensed phase.

**Acknowledgment.** This work was supported by National Science Foundation Grant CHE-8957243. B.M.H. acknowledges support of a Deutsche Forschungsgemeinschaft fellowship. We thank Dr. Timothy Lee for providing us the results of unpublished calculations and for several helpful discussions.

## References and Notes

- (1) Cotton, F. A.; Wilkinson, G. *Advanced Inorganic Chemistry*; John Wiley and Sons: New York, 1988; Chapter 10.
- (2) Fehsenfeld, F. C.; Howard, C. J.; Schmeltekopf, A. L. *J. Chem. Phys.* **1975**, *63*, 2835.
- (3) Nguyen, M.-T.; Hegarty, A. F. *J. Chem. Soc. Perkin Trans. 2* **1984**, 2043.
- (4) (a) Cacace, F.; Attinà, M.; de Petris, G.; Speranza, M. *J. Am. Chem. Soc.* **1989**, *111*, 5481. (b) Cacace, F.; Attinà, M.; de Petris, G.; Speranza, M. *J. Am. Chem. Soc.* **1990**, *112*, 1014.
- (5) Lee, T. J.; Rice, J. E. *J. Phys. Chem.* **1992**, *96*, 650.
- (6) Sunderlin, L. S.; Squires, R. R. *Chem. Phys. Lett.* **1993**, *212*, 307.
- (7) Cacace, F.; Attinà, M.; de Petris, G.; Speranza, M. *J. Am. Chem. Soc.* **1994**, *116*, 6413.
- (8) Hanson, D.; Ravishankara, A. R. *J. Phys. Chem.* **1992**, *96*, 2682.
- (9) Leu, M.-T.; Moore, S. B.; Keyser, L. F. *J. Phys. Chem.* **1991**, *95*, 7763.
- (10) Molina, M. J.; Tso, T.-L.; Molina, L. T.; Wang, F. C.-Y. *Science* **1987**, *238*, 1253.
- (11) Solomon, S.; Garcia, R. R.; Rowland, F. S.; Wuebbles, D. J. *Nature* **1986**, *321*, 755.
- (12) Tolbert, M. A.; Rossi, M. J.; Malhotra, R.; Golden, D. M. *Science* **1987**, *238*, 1258.
- (13) Atkinson, R.; Tuazon, E. C.; Mac Leod, H.; Aschmann, S. M.; Winer, A. M. *Geophys. Res. Lett.* **1986**, *13*, 117.
- (14) Wofsy, S. C.; Molina, M. J.; Salawitch, R. J.; Fox, L. E.; McElroy, M. B. *J. Geophys. Res.* **1988**, *93*, 2442.
- (15) Nelson, C. M.; Okumura, M. *J. Phys. Chem.* **1992**, *96*, 6112.
- (16) Lee, T. J.; Rice, J. E. *J. Phys. Chem.* **1993**, *97*, 6637.
- (17) Slanina, Z.; Uhlík, F.; Hinchliffe, A. *Spect. Lett.* **1994**, *27*, 563.
- (18) van Doren, J. M.; Viggiano, A. A.; Morris, R. A. *J. Am. Chem. Soc.* **1994**, *116*, 6957.
- (19) Schindler, T.; Berg, C.; Niedner-Schatteburg, G.; Bondybey, V. E. *J. Chem. Phys.* **1996**, *104*, 3998.
- (20) (a) Okumura, M.; Yeh, L. I.; Lee, Y. T. *J. Chem. Phys.* **1985**, *83*, 3705. (b) Yeh, L. I.; Okumura, M.; Myers, J. D.; Price, J. M.; Lee, Y. T. *J. Chem. Phys.* **1989**, *91*, 7319. (c) Price, J. M.; Crofton, M. W.; Lee, Y. T. *J. Phys. Chem.* **1991**, *95*, 2182. (d) Boo, D. W.; Lee, Y. T. *Chem. Phys. Lett.* **1993**, *211*, 358.
- (21) Yeh, L. I.; Price, J. M.; Lee, Y. T. *J. Am. Chem. Soc.* **1989**, *111*, 5597.
- (22) Cao, Y.; Choi, J.-H.; Haas, B.-M.; Johnson, M. S.; Okumura, M. *J. Chem. Phys.* **1993**, *99*, 9307.
- (23) Cao, Y.; Choi, J.-H.; Haas, B.-M.; Okumura, M. *J. Phys. Chem.* **1994**, *98*, 12176.
- (24) Choi, J.-H.; Kuwata, K. T.; Haas, B.-M.; Cao, Y.; Johnson, M. S.; Okumura, M. *J. Chem. Phys.* **1994**, *100*, 7153.
- (25) Schmeisser, M. *Inorg. Synth.* **1967**, *9*, 127.
- (26) Taylor, G. B. *Ind. Eng. Chem.* **1925**, *17*, 633.
- (27) Schack, C. J. *Inorg. Chem.* **1967**, *6*, 1938.
- (28) Benedict, W. S.; Gailar, N.; Plyler, E. K. *J. Chem. Phys.* **1956**, *24*, 1139.
- (29) Lee, T. J.; Rice, J. E. Personal communication.
- (30) Forney, D.; Thompson, W. E.; Jacox, M. E. *J. Chem. Phys.* **1993**, *99*, 7393.
- (31) Junttila, M.-L.; Lafferty, W. J.; Burkholder, J. B. *J. Mol. Spectrosc.* **1994**, *164*, 583.
- (32) Zhang, X.; Mereand, E. L.; Castleman, A. W., Jr. *J. Phys. Chem.* **1994**, *98*, 3554.
- (33) (a) Sodeau, J. R.; Horn, A. B.; Banham, S. F.; Koch, T. G. *J. Phys. Chem.* **1995**, *99*, 6258. (b) Koch, T. G.; Banham, S. F.; Sodeau, J. R.; Horn, A. B.; McCoustra, M. R. S.; Chesters, M. A. *J. Geophys. Res.* **1997**, *102*, 1513.
- (34) Hanson, D. R. *J. Phys. Chem.* **1995**, *99*, 13059.
- (35) Burley, J. D.; Johnston, H. S. *Geophys. Res. Lett.* **1992**, *19*, 1359.
- (36) Robinson, G. N.; Worsnop, D. R.; Jayne, J. T.; Kolb, C. E.; Davidovits, P. *J. Geophys. Res.* **1997**, *102*, 3583.